Kohn anomalies in superconductors

Michael E. Flatté
Institute for Theoretical Physics, University of California, Santa Barbara, California 93106-4030
(Received 14 May 1993; revised 10 February 1994)

The detailed behavior of phonon dispersion curves near momenta which span the electronic Fermi sea in a superconductor is presented. An anomaly, similar to the metallic Kohn anomaly, exists in a superconductor's dispersion curves when the frequency of the phonon spanning the Fermi sea exceeds twice the superconducting energy gap. This anomaly occurs at approximately the same momentum but is *stronger* than the normal-state Kohn anomaly. It also survives at finite temperature, unlike the metallic anomaly. Determination of Fermi-surface diameters from the location of these anomalies, therefore, may be more successful in the superconducting phase than in the normal state. However, the superconductor's anomaly fades rapidly with increased phonon frequency and becomes unobservable when the phonon frequency greatly exceeds the gap. This constraint makes these anomalies useful only in high-temperature superconductors such as $La_{1.85}Sr_{0.15}CuO_4$.

I. INTRODUCTION

The Kohn anomaly[1] occurs in a metal's phonon dispersion curves when a phonon's momentum spans the Fermi surface. Locating these anomalies through inelastic neutron scattering (on lead[2] or niobium,[3] for example) and inelastic helium scattering (on a platinum surface[4]), accurately measures the Fermi surface, as well as the electron-phonon interaction. This paper consists of a derivation and discussion of a similar type of anomaly, with greater magnitude, which exists in a superconductor. This anomaly could prove useful in $La_{1.85}Sr_{0.15}CuO_4$, whose Fermi-surface shape generates heated debate.

A significant decay product of a phonon in a metal is a single electron-hole pair. The Kohn anomaly occurs because, for momenta smaller than the Fermi surface diameter, there exist single-pair excitations of the electron gas for the phonon to decay into, while for larger momenta there are none. This sharp change in the availability of decay products causes a nonanalyticity in the phonon's lifetime and frequency. The sharpness originates in the discontinuous electron occupation at the Fermi surface at 0 K. Thus, even in an interacting electron gas, with a quasiparticle weight less than unity, the anomaly persists. The discontinuity vanishes at finite temperature,[5] resulting in a phonon anomaly smoothed over the momentum range $k_BT/\hbar v_F$, where v_F is the Fermi velocity. This smoothing is typically unobservable. A standard approximation in the derivation of the metallic anomaly is the use of the *static* pair response function. Neglecting the phonon frequency is suggested by the smoothness of the metal's electronic response function at frequencies much smaller than the Fermi energy ϵ_F. This smoothness persists at finite temperature, also justifying a static approximation.

Section II predicts some unusual metallic Kohn anomalies in the high-temperature superconductor $La_{2-x}Sr_xCuO_4$. First, at room temperatures, evidence is presented that any Kohn anomaly would be substantially smoothed. This may explain the failure of a search[6] for Kohn anomalies in $La_{2-x}Sr_xCuO_4$. Second, the static approximation for the pair response function is shown to be inadequate and new momentum locations for Kohn anomalies are predicted.

A further failure of the static approximation is explored in Sect. III, devoted to Kohn anomalies in superconductors. In most superconductors the energy gap Δ produces substantial structure in the pair response function at frequencies much less than phonon frequencies ($\Delta \ll \hbar\omega_D$). Thus the static electronic response differs qualitatively from that at a phonon's frequency. The fundamental conclusion is that Kohn anomalies may survive in superconductors, even at finite temperature. The effects predicted in this work are expected to be unobservable in low-temperature superconductors.

Figures 1(a) and 1(b) illuminate the two types of anomalies which occur in a superconductor. Figure 1(a) shows the minimum-energy electronic excitations (from now on, the adjective "single-pair" will be dropped) for a two- or three-dimensional isotropic-gap superconductor (solid line) and normal metal (dashed line). In Fig. 1(b) the region near $q = 2k_F$ has been enlarged so that the solid and dashed lines can be distinguished. For the superconductor, in the region to the left of and above the solid line there exist excitations, so the electronic response function has a finite imaginary component. To the right of and below the solid line, however, no excitations exist, so the response function is real. A function must be nonanalytic on the border between a region where it is identically zero and a region where it is nonzero; the imaginary part of the response function is nonanalytic on this (solid) line. By Kramers-Kronig relations, the real part is nonanalytic there as well. Thus the superconductor must produce an anomaly in phonon dispersion curves at $q \sim 2k_F$ when $\hbar\omega(2k_F) > 2\Delta$. All phonons

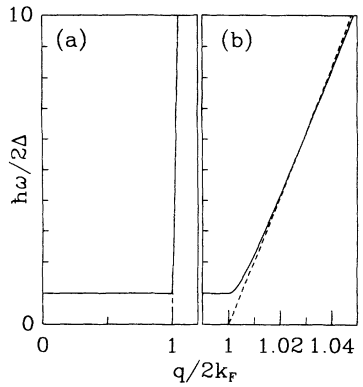

FIG. 1. Minimum single-pair excitation energy in a two- or three-dimensional isotropic-gap superconductor (solid line) and normal metal (dashed line). Here $2\Delta/\hbar k_F v_F = 0.01$. (a) Full range of momentum q. (b) Closeup of the region near $q = 2k_F$.

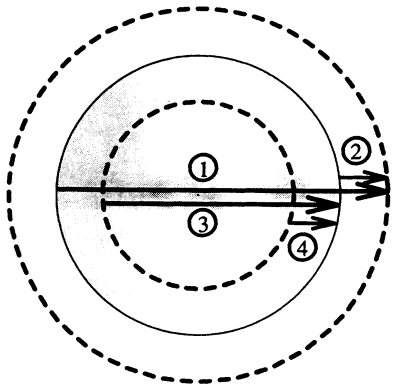

FIG. 2. Four possible extremal excitations for a fixed ω. The two dashed lines are energy contour surfaces at $\hbar\omega$ below and above the Fermi surface, indicated by the solid circle. For momenta greater than (1) and (3) there are no real single-pair excitations of the Fermi sea of this type. For momenta smaller than (2) and (4) there are no single-pair excitations of this type.

resolvable by neutron scattering in low-temperature superconductors satisfy this condition as do most in high-temperature ones.

The anomalies in phonon dispersion curves in superconductors for $q < 2k_F$ and $\hbar\omega = 2\Delta$ were proposed by Bobetic,[7] elaborated by Schuster,[8] and observed in Nb_3Sn (Ref. 9) and niobium.[10] This work will only consider the anomalies induced in phonon dispersion curves crossing the solid line when $q \sim 2k_F$.

Numerical calculations of the effect of d-wave and s-wave superconductivity on phonon lifetimes and frequencies have been performed for a nearest-neighbor tight-binding model by Marsiglio.[11] The primary concern of Ref. 11 was to locate features identifying nesting, or which distinguish s-wave from d-wave gaps. The results presented here concern the location and analytic form of the anomalies. The appearance of Kohn anomalies does not depend on nesting, merely the diameter of the Fermi surface. As discussed in Sec. V, the analytic form of the Kohn anomalies is identical for s-wave and d-wave gaps for almost all phonon momenta.

II. NORMAL STATE

Kohn anomalies in materials where the ratio of the phonon energy scale to the electronic energy scale, $2\omega/k_F v_F$, is small but not negligible are discussed now.

The metal's electron-hole response function,

$$P_M(\mathbf{q},\omega) = \lim_{\alpha\to 0}\sum_{\mathbf{k}} \frac{f(\epsilon_{\mathbf{k}}) - f(\epsilon_{\mathbf{k}+\mathbf{q}})}{\epsilon_{\mathbf{k}} - \epsilon_{\mathbf{k}+\mathbf{q}} - \hbar\omega - i\alpha}, \qquad (2.1)$$

depends on the ratio $2\omega/k_F v_F$. Here $f(\epsilon)$ is the Fermi function and $\epsilon_{\mathbf{k}}$ the dispersion relation for the metal's electrons. The response in Eq. (2.1) for a spherical Fermi surface in three dimensions is the Lindhard function:

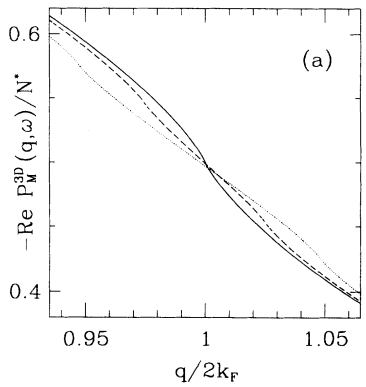

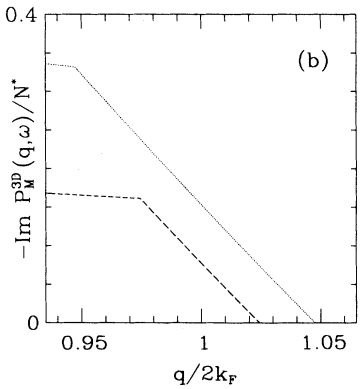

FIG. 3. $-P_M^{3D}(\mathbf{q},\omega)/N^*$ for $2\omega/k_F v_F = 0$ (solid line), 0.1 (dashed line), and 0.2 (dotted line). (a) Real part. (b) Imaginary part. The solid line is not visible in (b) because $\mathrm{Im}P_M(q,0) = 0$.

$$P_M^{3D}(\mathbf{q},\omega) = -\frac{N^*}{4x}\left(2x - \frac{(1-[x+\nu]^2)}{2}\ln\left|\frac{1-x-\nu}{1+x+\nu}\right| - \frac{(1-[x-\nu]^2)}{2}\ln\left|\frac{1-x+\nu}{1+x-\nu}\right| - \frac{i\pi}{2}\left[\theta(1-|x+\nu|)(1-[x+\nu]^2) - \theta(1-|x-\nu|)(1-[x-\nu]^2)\right]\right), \quad (2.2)$$

where $x = q/2k_F$, $\nu = m\omega/\hbar q k_F$, N^* is the density of states at the Fermi surface, and θ is the Heavyside step function. In the limit $2\omega/k_F v_F \to 0$ ($\nu \to 0$),

$$P_M^{3D}(\mathbf{q},0) = -\frac{N^*}{4x}\left(2x - (1-x^2)\ln\left|\frac{1-x}{1+x}\right|\right). \quad (2.3)$$

The location of the Kohn anomaly at the momentum $2k_F$ follows directly from the nonanalyticity of the right-hand side of Eq. (2.3) at that momentum. Clearly from Eq. (2.2), however, at finite frequency the nonanalyticity takes place at

$$q_\pm = k_F \pm k_F\sqrt{1-\frac{2\omega}{k_F v_F}} \sim 2k_F \pm \frac{\omega}{v_F}. \quad (2.4)$$

Figure 2 indicates the four types of extremal excitations which produce anomalies in the response function. Excitation (1) takes an electron from the Fermi surface and places it in a state $\hbar\omega$ above the Fermi surface on the other side of the Fermi sea. Excitation (3) takes an electron from a state $\hbar\omega$ below the Fermi surface and places it on the Fermi surface on the other side. For momenta greater than (1) or (3) these types of excitations do not exist. This explains the origin of the two solutions for $q_\pm$. For $\hbar\omega \approx 0$, excitations (1) and (3) are the same. The static approximation succeeds because the nonanalyticity has the same form for finite frequency as for zero frequency and because the differences in $q_\pm$ cannot be resolved. Excitations (2) and (4) concern the zero-momentum anomaly in a metal's response function which will not be discussed in this work.

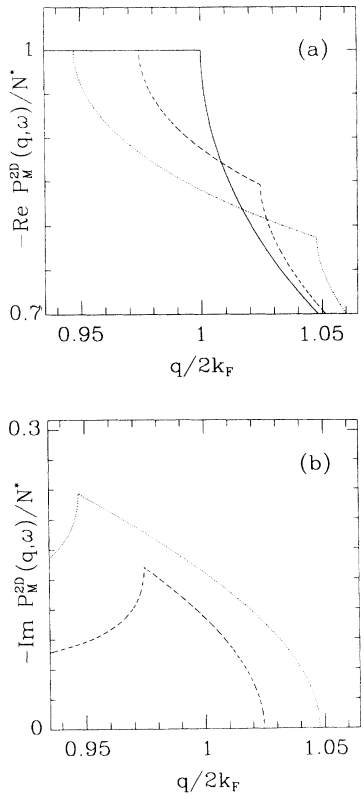

FIG. 4. $-P_M^{2D}(\mathbf{q},\omega)/N^*$ for $2\omega/k_F v_F = 0$ (solid line), 0.1 (dashed line), and 0.2 (dotted line). (a) Real part. (b) Imaginary part.

Figure 3 shows $P_M^{3D}(\mathbf{q},\omega)$ for various values of $2\omega/k_F v_F$. These are plotted to indicate the changes in the anomalies' momenta due to finite frequencies. In a high-temperature superconductor, where the bandwidth may be less than an electron volt and the phonon energies are tens of meV, the splitting evident in Eq. (2.4) may be observable.

Another feature of the high-temperature superconductors is that their electronic structure is quasi-two-dimensional. In two dimensions the slope of the response function[12] is discontinuous and divergent at $q_\pm$:

$$P_M^{2D}(\mathbf{q},\omega) = -\frac{N^*}{2x}\left(2x - \mathrm{sgn}(x+\nu)\theta(|x+\nu|-1)\sqrt{(x+\nu)^2-1} - \mathrm{sgn}(x-\nu)\theta(|x-\nu|-1)\sqrt{(x-\nu)^2-1} - i\theta(1-|x+\nu|)\sqrt{1-(x+\nu)^2} + i\theta(1-|x-\nu|)\sqrt{1-(x-\nu)^2}\right). \quad (2.5)$$

The two-dimensional response contains stronger nonanalyticities than the three-dimensional response. If the c-axis dispersion of a high-temperature superconductor is small compared to phonon frequencies, which is typically the case, the Kohn anomalies will appear to have the nonanalyticities associated with a two-dimensional system. Figure 4 shows $P_M^{2D}(\mathbf{q},\omega)$ for various values of $2\omega/k_F v_F$.

Figures 5 and 6 indicate the location of Kohn anomalies in $(\mathbf{q},\omega)$ space in the (100) and (110) directions for $La_{1.85}Sr_{0.15}CuO_4$, using the two-dimensional Fermi-surface parametrizations of Hybertsen *et al.*[13] The low-energy phonons are also plotted as the solid lines.[14] Every time a dispersion curve crosses one of these lines, a Kohn anomaly should appear. In the (100) direction the difference in momentum between the actual anomaly and the static anomaly may be visible in high-energy phonons. An experiment[6] looking for Kohn anomalies in

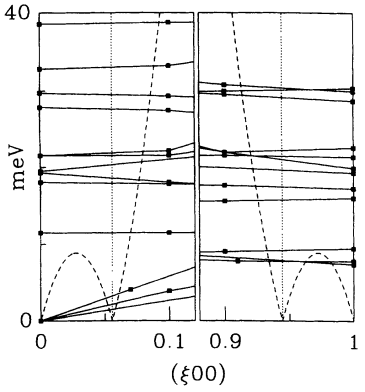

FIG. 5. Kohn anomalies for phonons with momenta parallel to the (100) direction in $La_{1.85}Sr_{0.15}CuO_4$. Points on the dashed line correspond to Kohn anomalies when phonon curves cross them. Solid squares are the low-energy phonons from Ref. 14, solid lines are a guide to the eye. The dotted line indicates the momentum of the static anomaly.

$La_{1.9}Sr_{0.1}CuO_4$ was performed at temperatures too high to see this splitting ($k_BT > \hbar\omega$) and probably too high ($2k_BT/\hbar k_F v_F \sim 0.1$) to see anomalies at all.

If the Fermi surface had the form of small isolated pockets, as seen in some t-J models, there would be anomalies at momenta connecting the insides and outsides of these pockets as well as spanning the pockets themselves. The large-momenta anomalies connecting pockets would only occur in certain directions (depending on the details of the model). Thus the anomalies seen would differ substantially for a pocket Fermi surface versus a "large" Fermi surface.

III. KOHN ANOMALIES IN SUPERCONDUCTORS

A. $\hbar\omega < 2\Delta$

The disappearance of the Kohn anomaly in a superconductor was suggested by Hurault[15] as a manifestation of Fermi-surface smoothing in a superconductor. The quasiparticle description, due to Bogoliubov, provides the most convenient method of calculating the effect of the superconducting electron system on the phonons.[16] The quasiparticle creation and annihilation operators $\gamma^\dagger, \gamma$ relate to the electron creation and annihilation operators $c^\dagger, c$ as follows:

$$\gamma^\dagger_{\mathbf{k},\uparrow} = u_{\mathbf{k}} c^\dagger_{\mathbf{k},\uparrow} - v_{\mathbf{k}} c_{-\mathbf{k},\downarrow} ,$$
$$\gamma_{-\mathbf{k},\downarrow} = u_{\mathbf{k}} c_{-\mathbf{k},\downarrow} + v_{\mathbf{k}} c^\dagger_{\mathbf{k},\uparrow} . \tag{3.1}$$

Here

$$u_{\mathbf{k}} = \frac{1}{\sqrt{2}}\left(1 + \frac{\epsilon_{\mathbf{k}}}{E_{\mathbf{k}}}\right)^{\frac{1}{2}}, \qquad v_{\mathbf{k}} = \frac{1}{\sqrt{2}}\left(1 - \frac{\epsilon_{\mathbf{k}}}{E_{\mathbf{k}}}\right)^{\frac{1}{2}}, \tag{3.2}$$
$$u_{\mathbf{k}} v_{\mathbf{k}} = \frac{\Delta}{2E_{\mathbf{k}}},$$

where $E_{\mathbf{k}} = \sqrt{\epsilon^2_{\mathbf{k}} + \Delta^2}$ is the energy added to the system by creating a quasiparticle of momentum $\mathbf{k}$. The Hamiltonian, expressed in quasiparticle operators, is then

$$H_o = \sum_{\mathbf{k},s} E_{\mathbf{k}} \gamma^\dagger_{\mathbf{k},s} \gamma_{\mathbf{k},s} \tag{3.3}$$

and the ground state contains no quasiparticles.

A significant difference between the superconducting system and the normal system is the $v_{\mathbf{k}}$ function, which is an analogue of the Fermi occupation function $f(\epsilon_{\mathbf{k}})$ in a metal. At zero temperature $f(\epsilon_{\mathbf{k}})$ has a discontinuity at the Fermi momentum, while $v_{\mathbf{k}}$ smoothly falls to zero over a momentum range $(\hbar/\xi)$. $v_{\mathbf{k}}$ and $f(\epsilon_{\mathbf{k}})$ are shown in Fig. 7. The normal-metal Kohn anomaly arises from the discontinuity in the electron occupation, and as $f(\epsilon_{\mathbf{k}})$ becomes smoother due to increased temperature, the apparent anomaly becomes weaker.[5]

In work primarily devoted to calculating the screening around a static impurity, Hurault[15] suggested that the smoothness of $v_{\mathbf{k}}$ due to superconductivity affected the Kohn anomaly the same way as the smoothness of $f(\epsilon_{\mathbf{k}})$ at finite temperature affected the normal-metal anomaly.

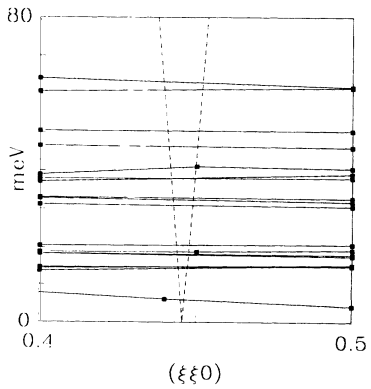

FIG. 6. Same as Fig. 5 except for phonons with momenta parallel to the (110) direction.

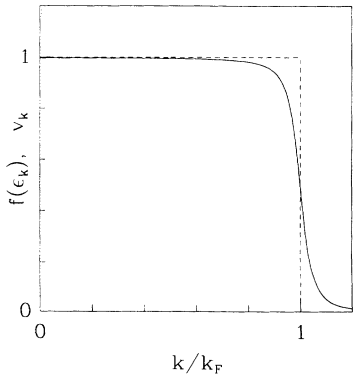

FIG. 7. Occupation number $f(\epsilon_{\mathbf{k}})$ for a normal metal at 0 K (dashed line) and the function $v_{\mathbf{k}}$ for a superconductor at 0 K (solid line).

He concluded that a superconductor has no true Kohn anomaly. The Kohn anomaly would be "smoothed" over a momentum range of $(\hbar/\xi)$.

This heuristic explanation needs to be reexamined in the light of the existence of anomalies for higher phonon frequencies, pointed out in Sec. I. The Fermi-surface sharpness cannot change as a function of frequency in the superconductor. Instead, the explanation for the smoothing of the Kohn anomaly at small frequencies must be due to the lack of *any* electronic excitations in the superconductor, at small *or* large momenta [as seen in Figs. 1(a) and 1(b)].

Calculating the nonanalytic behavior of an anomaly at finite frequency is necessary to make this argument concrete. The superconducting electronic response function is

$$P_S(\mathbf{q},\omega)=\lim_{\alpha\to 0}\sum_{\mathbf{k}}\left(\frac{E_{\mathbf{k}}E_{\mathbf{q}-\mathbf{k}}-\epsilon_{\mathbf{k}}\epsilon_{\mathbf{q}-\mathbf{k}}+\mathrm{Re}(\Delta_{\mathbf{k}}\Delta^*_{\mathbf{q}-\mathbf{k}})}{2E_{\mathbf{k}}E_{\mathbf{q}-\mathbf{k}}}\right)\frac{-1}{E_{\mathbf{k}}+E_{\mathbf{q}-\mathbf{k}}-\hbar\omega-i\alpha}, \tag{3.4}$$

where the sum is over *all* $\mathbf{k}$ values. The parenthetical factor, called the coherence factor and denoted $C(\mathbf{k},\mathbf{q}-\mathbf{k})$, reaches its maximum of 1 for $\mathbf{k}$ and $\mathbf{q}-\mathbf{k}$ at the Fermi surface and $\Delta_{\mathbf{k}}\Delta^*_{\mathbf{q}-\mathbf{k}}$ real and positive. It behaves similarly to the occupation expression $f(\epsilon_{\mathbf{k}})-f(\epsilon_{\mathbf{k}+\mathbf{q}})$ in the normal metal's response function, Eq. (2.1), but while the occupation expression vanishes sharply as a function of $\mathbf{k}$ or $\mathbf{q}$, C decays to zero with a scale given by the inverse coherence length. Therefore C is the component of $P_S(\mathbf{q},\omega)$ which simulates the behavior of finite temperature. For the rest of this section, the gap will be assumed isotropic. Section V will discuss anisotropic gaps.

The second factor of Eq. (3.4), the energy denominator, has poles for all excitations of the Bogoliubov quasiparticle sea. The imaginary part of $P_S(\mathbf{q},\omega)$ consists of contributions from each of these poles (the coherence factor is real).

At zero frequency there are no excitations in the isotropic superconductor. Since there are no poles of the energy denominator, $P_S(\mathbf{q},\omega)$ is real for all $\mathbf{q}$. The smoothness of the integrand in Eq. (3.4) with respect to $\mathbf{q}$ for all values of $\mathbf{k}$ forces the response function to be smooth with respect to $\mathbf{q}$.

This smoothness can be estimated in a simple way from the change of $P_S(\mathbf{q},\omega)$ at $q=2k_F$. In three dimensions the sum from Eq. (3.4) can be replaced by the following integral:

$$P_S^{3\mathrm{D}}(\mathbf{q},0)=-\left(\frac{m}{2qk_F\hbar^2}\right)N^*\int_{-\epsilon_F}^{\infty}d\epsilon\int_{\frac{\hbar^2(k-q)^2}{2m}}^{\frac{\hbar^2(k+q)^2}{2m}}\times d\epsilon'\frac{EE'-\epsilon\epsilon'+\Delta^2}{2EE'(E+E')}. \tag{3.5}$$

Here $E=\sqrt{\epsilon^2+\Delta^2}$ and N^* is the density of states per unit energy at the Fermi energy in an otherwise identical material with $\Delta=0$. The integral in Eq. (3.5) can be estimated near $q=2k_F$ to yield a measure of the remnant of the anomaly:

$$2k_F\frac{\partial P_S^{3\mathrm{D}}(\mathbf{q},0)}{\partial q}\bigg|_{2k_F}\Big/P_S^{3\mathrm{D}}(2\mathbf{k_F},0)\sim 2\ln\left(\frac{2\Delta}{k_Fv_F}\right)\sim 2\ln\left(\frac{2}{k_F\xi}\right). \tag{3.6}$$

When Δ vanishes, the logarithmically divergent slope of the normal-metal response reemerges. That response, the Lindhard function, is Eq. (2.2).

For finite but small frequencies in the superconductor, the slope magnitude increases to

$$\left|2k_F\frac{\partial P_S^{3\mathrm{D}}(\mathbf{q},\omega)}{\partial q}\bigg|_{2k_F}\Big/P_S^{3\mathrm{D}}(2\mathbf{k_F},0)\right|\sim\ln\left(\frac{(k_Fv_F)^2}{(2\Delta)^2-(\hbar\omega)^2}\right). \tag{3.7}$$

This increases results from the overall decrease in all the energy denominators in Eq. (3.4), due to a finite driving frequency. That change increases the contribution of each virtual excitation to the response of the superconductor. The overall response of the superconductor also increases, so the relative magnitude of the slope does not change for small but finite frequency:

$$\left|2k_F\frac{\partial P_S^{3\mathrm{D}}(\mathbf{q},\omega)}{\partial q}\bigg|_{2k_F}\Big/P_S^{3\mathrm{D}}(2\mathbf{k_F},\omega)\right|\sim 2\ln\left(\frac{2\Delta}{k_Fv_F}\right)\sim 2\ln\left(\frac{2}{k_F\xi}\right). \tag{3.8}$$

In a quasi-two-dimensional superconductor a similar effect occurs. Instead of diverging as in Eq. (2.5), however, the slope magnitude reaches a maximum value of

$$\left|2k_F\frac{\partial P_S^{2\mathrm{D}}(\mathbf{q},\omega)}{\partial q}\bigg|_{2k_F}\Big/P_S^{2\mathrm{D}}(2\mathbf{k_F},\omega)\right|\sim\left(\frac{k_Fv_F}{2\Delta}\right)^{\frac{1}{2}}. \tag{3.9}$$

In one dimension the response-function magnitude reaches a maximum of

$$|P_S^{1\mathrm{D}}(2\mathbf{k_F},\omega)|\sim\frac{N^*}{4}\ln\left(\frac{(k_Fv_F)^2}{(2\Delta)^2-(\hbar\omega)^2}\right), \tag{3.10}$$

whereas in the normal metal it diverges logarithmically:

$$P_M^{1D}(\mathbf{q},\omega) = N^*\left\{\frac{1}{4x}\ln\left|\frac{(1-x)^2-\nu^2}{(1+x)^2-\nu^2}\right| + \frac{i\pi}{4x}[\theta(1-|x+\nu|)-\theta(1-|x-\nu|)]\right\}. \tag{3.11}$$

These results are quite similar mathematically to Hurault's. The disagreement comes in attributing the lack of an anomaly to the smooth functional behavior of the coherence factor. In the next section nonanalyticities will be discussed in $P_S(\mathbf{q},\omega)$ which give rise to Kohn anomalies. The coherence factor will not be changed. It will be the existence of poles in the sum in Eq. (3.4) which changes the results. An appropriate analogy would be to a semiconductor, where for frequencies less than the energy gap there could be no anomaly, while for frequencies greater than the energy gap anomalies could exist. The next section deals with $2\Delta < \hbar\omega$, a much more common occurrence than $\hbar\omega < 2\Delta$.

B. $2\Delta \lesssim \hbar\omega$

When the phonon energy exceeds the excitation gap, the superconductor recovers an anomaly. For $q > 2k_F$ the minimum-energy quasiparticle mode creates two quasiparticles with momentum $q/2 > k_F$. Because both of these quasiparticles are created with a momentum greater than the Fermi momentum, this mode does not have an analogy in the normal state. The superconductor, therefore, has lower energy excitations at high q than the normal metal, as can be seen in Fig. 1(b).

For a fixed $\hbar\omega > 2\Delta$ there are two regimes of q, separated by the solid line in Figs. 1(a) and 1(b). For small q, $\mathrm{Im}P_S(\mathbf{q},\omega) \neq 0$ because the minimum excitation energy is less than the driving frequency. For large q no excitable modes of the electron gas exist, so $\mathrm{Im}P_S(\mathbf{q},\omega) = 0$. Therefore, the imaginary part of $P_S(\mathbf{q},\omega)$, and by implication from the Kramers-Kronig relations the real part as well, cannot be analytic functions of q. The momentum $q_c(\omega)$ beyond which no modes of frequency ω or less exist is the anomaly's momentum. A *nonspherical* Fermi surface does not affect the analytic form of the anomalies. If the Fermi surface is known, the anomalies' momenta in various directions can be calculated. I will now derive the form of the nonanalyticity of $P_S(\mathbf{q},\omega)$ at $q = q_c(\omega)$.

The nonanalyticity in $P_S(\mathbf{q},\omega)$ at $q = q_c(\omega)$ can be extracted by expanding the energy denominator in Eq. (3.4) around the anomaly's momentum:

$$E_{\mathbf{k}} + E_{\mathbf{q}-\mathbf{k}} = 2E_{\mathbf{q}_c/2} + \frac{\epsilon_{\mathbf{q}_c/2}(p^2 - q_c^2/4) + \epsilon_{\mathbf{q}_c/2}(p^2 + q^2 + 2pq\cos\theta - q_c^2/4)}{2mE_{\mathbf{q}_c/2}/\hbar^2}. \tag{3.12}$$

This expansion is valid when the quantities in parentheses are small compared to $\hbar\omega/2$, which will usually mean small compared to Δ. This expansion, therefore, is only valid for states $\mathbf{k}$ and $\mathbf{q}-\mathbf{k}$ in a region of diameter $(\hbar/\xi)$ around the momentum $\mathbf{q}_c/2$. Consider the sum in Eq. (3.4) to be restricted to this region. An evaluation of that sum, which will follow and will be called $\tilde{P}_S(\mathbf{q},\omega)$, accurately gives $\mathrm{Im}P_S(\mathbf{q},\omega)$ and the nonanalytic part of $\mathrm{Re}P_S(\mathbf{q},\omega)$ near the nonanalyticity at $q = q_c$.

Since $2E_{\mathbf{q}_c/2} = \hbar\omega$ and the coherence factor is smooth over a momentum $(\hbar/\xi)$, the sum can be written as the following integrals in one, two, and three dimensions:

$$\tilde{P}_S^{1D}(\mathbf{q},\omega) = -N^*\frac{\hbar\omega}{\epsilon_{\mathbf{q}_c}/2}\frac{k_F}{4}C\left(\frac{\mathbf{q}}{2},\frac{\mathbf{q}}{2}\right) \times \int_{\frac{q_c}{2}-a}^{\frac{q_c}{2}+a}\frac{dp}{2p^2 - q_c^2/2 + q^2 - 2pq}, \tag{3.13}$$

$$\tilde{P}_S^{2D}(\mathbf{q},\omega) = -N^*\frac{\hbar\omega}{\epsilon_{\mathbf{q}_c/2}}\frac{q_c}{8\pi}C\left(\frac{\mathbf{q}}{2},\frac{\mathbf{q}}{2}\right) \times \int_{\frac{q_c}{2}-a}^{\frac{q_c}{2}+a}\int_{\pi-\frac{a}{k_F}}^{\pi+\frac{a}{k_F}} \times \frac{dpd\theta}{2p^2 - q_c^2/2 + q^2 + 2pq\cos\theta}, \tag{3.14}$$

$$\tilde{P}_S^{3D}(\mathbf{q},\omega) = -N^*\frac{\hbar\omega}{\epsilon_{\mathbf{q}_c/2}}\frac{q_c^2}{8k_F}C\left(\frac{\mathbf{q}}{2},\frac{\mathbf{q}}{2}\right) \times \int_{\frac{q_c}{2}-a}^{\frac{q_c}{2}+a}\int_{\pi-\frac{a}{k_F}}^{\pi}\frac{dpd\cos\theta}{2p^2 - q_c^2/2 + q^2 + 2pq\cos\theta}, \tag{3.15}$$

where a is a cutoff of order ξ^{-1}.

Evaluating the integrals above in the limit $q \to q_c$ and defining $\tilde{q} = q - q_c$ yields the following forms for the response functions:

$$\tilde{P}_S^{1D}(\mathbf{q},\omega) = -iN^*\frac{\hbar\omega}{\epsilon_{\mathbf{q}_c/2}}\left[\frac{\pi k_F}{8\sqrt{-q_c\tilde{q}}}\right]C\left(\frac{\mathbf{q}}{2},\frac{\mathbf{q}}{2}\right), \quad \tilde{q} < 0$$
$$= -N^*\frac{\hbar\omega}{\epsilon_{\mathbf{q}_c/2}}\left[\frac{\pi k_F}{8\sqrt{q_c\tilde{q}}}\right]C\left(\frac{\mathbf{q}}{2},\frac{\mathbf{q}}{2}\right), \quad \tilde{q} > 0, \tag{3.16}$$

$$\tilde{P}_S^{2D}(\mathbf{q},\omega) = N^*\frac{\hbar\omega}{\epsilon_{\mathbf{q}_c/2}}\frac{1}{4}\left[\ln\left|\frac{\tilde{q}q_c}{8a^2}\right| - i\pi\theta(-\tilde{q})\right]C\left(\frac{\mathbf{q}}{2},\frac{\mathbf{q}}{2}\right), \tag{3.17}$$

$$\tilde{P}_S^{3D}(\mathbf{q},\omega) = -N^*\frac{\hbar\omega}{\epsilon_{\mathbf{q}_c/2}}\left[P + i\pi\left(\frac{-\tilde{q}q_c}{32k_F^2}\right)^{\frac{1}{2}}\right]C\left(\frac{\mathbf{q}}{2},\frac{\mathbf{q}}{2}\right), \quad \tilde{q} < 0$$
$$= -N^*\frac{\hbar\omega}{\epsilon_{\mathbf{q}_c/2}}\left[P + \pi\left(\frac{\tilde{q}q_c}{32k_F^2}\right)^{\frac{1}{2}}\right]C\left(\frac{\mathbf{q}}{2},\frac{\mathbf{q}}{2}\right), \quad \tilde{q} > 0. \tag{3.18}$$

Here θ is the Heavyside step function and P is an uninteresting constant. Only $\tilde{P}_S^{1D}(2\mathbf{k_F},\omega)$ has been reported elsewhere.[11] The change in form of the integrals in Eqs. (3.13)– (3.15) when q passes through q_c causes the nonanalyticities in Eqs. (3.16)–(3.18).

The forms of these nonanalyticities differ from those in the normal metal. One origin for differences is the different dispersion of excitations with momentum near q_c in the metal versus the superconductor. In a normal metal, for finite frequency, the anomaly's momentum connects electronic states with different velocities. One electronic state rests on the Fermi surface and one does not. In the superconductor the two quasiparticle states have the same velocity, causing an amplification of the density of states for $E_{\mathbf{k}} + E_{\mathbf{q}-\mathbf{k}} = \hbar\omega$ and a *stronger* nonanalyticity. Another source of difference is the prefactor in Eqs. (3.16)–(3.18),

$$\frac{\hbar\omega}{\epsilon_{\mathbf{q}_c/2}} = \frac{1}{2}\left(1 - \left[\frac{2\Delta}{\hbar\omega}\right]^2\right)^{-\frac{1}{2}}, \tag{3.19}$$

which is due to the square-root divergence near the Fermi surface in the superconducting density of states. This also enhances the anomaly.

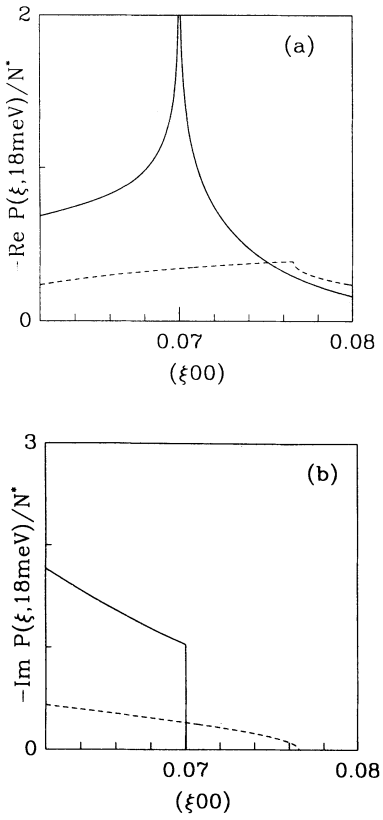

FIG. 8. Response function for a model of $La_{1.85}Sr_{0.15}CuO_4$ with the correct curvature at the points where a vector in the (100) direction spans the Fermi surface. The Fermi velocity was taken from Ref. 13. The frequency is fixed at 18 meV. The dashed line is for the normal metal and the solid line is for the superconductor. The nonanalyticities in these curves correspond to momenta where a phonon at this frequency would cross a pair-production threshold surface shown in Fig. 9. (a) Real part. (b) Imaginary part.

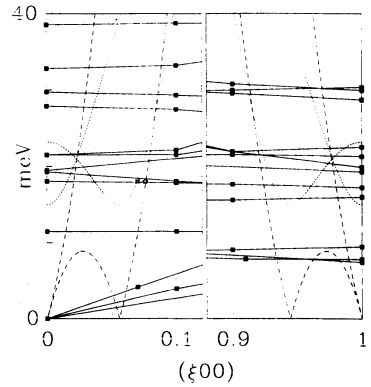

FIG. 9. Pair-production threshold in the superconductor (dotted line) in the (100) direction is shown on the same graph as the threshold in the normal metal (dashed line, previously shown in Fig. 5). The gap magnitude is taken to be 7.5 meV. The four-pointed star indicates the momentum and energy of the superconductor's anomaly. The five-pointed star indicates the momentum and energy of the normal-metal anomaly.

C. $\hbar\omega \gg 2\Delta$

For large phonon frequencies, the anomaly's momentum exceeds twice the Fermi momentum by well over

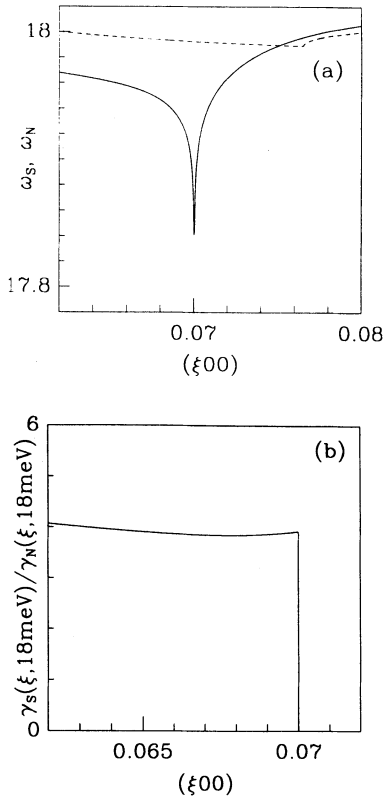

FIG. 10. Phonon dispersion curve near 18 meV in the normal and superconducting state of $La_{1.85}Sr_{0.15}CuO_4$. (a) Frequency. Dashed line: normal state; solid line: superconducting state. (b) Relative lifetime.

$(\hbar/\xi)$. In this case, the small value of the coherence factor $C(\frac{\mathbf{q_c}}{2}, \frac{\mathbf{q_c}}{2})$ renders the anomaly undetectable. A remnant of the normal-metal Kohn anomaly may still exist. Since all relevant excitations for this remnant are near the dashed line of Figs. 1(a) and 1(b), this situation is analogous to finite temperature in a normal metal. In the superconductor, phonons with momenta on both sides of the dashed line have real excitations, but the number of excitations decreases markedly, over a momentum range $(\hbar/\xi)$, upon crossing that dashed line. This would appear like the anomaly in the normal metal with a temperature of $T_{\text{effective}} \sim \Delta/k_B$.

IV. EXPERIMENTAL IMPLICATIONS

The actual size of the phonon anomalies can be estimated by including the response function in the phonon self-energy in the standard way[17] and then expanding about $\omega(2k_F) = \omega_o$:

$$\frac{\delta\omega(\mathbf{q})}{\omega_o} = \frac{\lambda\omega_o N^*}{2}\mathrm{Re}\left[\frac{\tilde{P}_S(\mathbf{q},\omega_o) - P_M(2\mathbf{k_F},\omega_o)}{N^*}\right], \quad (4.1)$$

where λ is the dimensionless electron-phonon coupling constant. The linewidth is simpler to express:

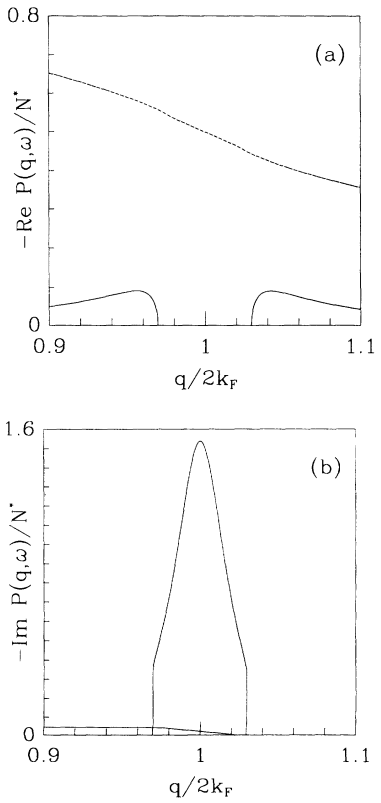

FIG. 11. Response function for a superconductor (solid line) and normal metal (dashed line) with a three-dimensional Fermi surface. $2\omega/k_F v_F = 0.1$ and $\hbar\omega/2\Delta = 1.25$. (a) Real part. (b) Imaginary part.

$$\frac{\gamma_S(\mathbf{q},\omega_o)}{\gamma_o} = \frac{\mathrm{Im}\tilde{P}_S(\mathbf{q},\omega_o)}{\mathrm{Im}P_M(2\mathbf{k_F},\omega_o)}. \quad (4.2)$$

In comparing anomaly magnitudes I will assume that λ in the superconductor equals the normal-metal value.

For $La_{1.85}Sr_{0.15}CuO_4$, the average value of λ over the whole Brillouin zone has been calculated[18] to be 1.37. The value of N^* has been calculated[19] to be 0.3/eV. Figure 8 shows the real and imaginary parts of the response function for the one-band model of $La_{1.85}Sr_{0.15}CuO_4$ used in Sec. II. The anomalies evident in Fig. 8 are due to crossing the pair threshold surfaces (shown for $La_{1.85}Sr_{0.15}CuO_4$ in Fig. 9). Figure 10 compares a phonon dispersion curve in the normal and superconducting state of $La_{1.85}Sr_{0.15}CuO_4$. Clearly the anomaly should be larger in superconducting $La_{1.85}Sr_{0.15}CuO_4$ than in metallic $La_{1.85}Sr_{0.15}CuO_4$. To show how the two-dimensional anomalies are much larger than the three-dimensional anomalies, Fig. 11 shows the metallic and superconducting response function for a three-dimensional spherical Fermi sea.

V. GAP ANISOTROPY

The primary effect of gap anisotropy is to make the quasiparticle pair threshold at $q \sim 2k_F$ different in different directions. The response functions Eqs. (3.16)–(3.18) can still be used if $\Delta_{\mathbf{q_c}/2}$ is substituted for Δ. An anisotropic gap also influences the Kohn anomalies through the coherence factor,

$$C\left(\frac{\mathbf{q_c}}{2}, \frac{\mathbf{q_c}}{2}\right) = \left(\frac{|\Delta_{\mathbf{q_c}/2}|}{E_{\mathbf{q_c}/2}}\right)^2, \quad (5.1)$$

which is independent of the phase of the gap for an inversion-symmetric Fermi surface and gap. This is markedly different from the anomalies where $q < 2k_F$, where gap magnitude *and* phase anisotropy[20,21] has a profound effect.

When the momentum spanning the Fermi surface connects two nodes in the gap the anomaly is weaker. This situation has been analyzed numerically by Marsiglio.[11]

VI. CONCLUSION

The vanishing of the Kohn anomaly for $\hbar\omega < 2\Delta$ results from the absence of electronic excitations at low energy in the superconductor rather than from a smoothing of the Fermi surface. The rapid decrease of the coherence factor of the minimum-energy excitation for $\hbar\omega \gg 2\Delta$ also eliminates the Kohn anomaly. A new regime exists when $2\Delta \lesssim \hbar\omega$; here superconductivity *enhances* the Kohn anomaly. An appropriate material to examine when looking for this effect would have phonon branches both above and below the excitation gap at $q \sim 2k_F$, as well as a quasi-two-dimensional electronic structure. High-T_c superconductors like $La_{1.85}Sr_{0.15}CuO_4$ are such

materials. Possible new effects in metallic Kohn anomalies have also been discussed.

Since an extremely sensitive probe of surface phonons exists in thermal-energy-inelastic-helium scattering,[4] I remark that similar arguments to those presented in this paper may apply to surface phonons.

ACKNOWLEDGMENTS

I would like to acknowledge useful conversations with W. Kohn, D. P. Clougherty, and D. J. Scalapino. This work was supported by the National Science Foundation under Grant No. PHY89-04035.

[1] W. Kohn, Phys. Rev. Lett. **2**, 393 (1959).
[2] B.N. Brockhouse *et al.*, Phys. Rev. **128**, 1099 (1962).
[3] R.I. Sharp, J. Phys. C **2**, 432 (1969).
[4] U. Harten, J.P. Toennies, C. Wöll, and G. Zhang, Phys. Rev. Lett. **55**, 2308 (1985).
[5] M.T. Béal-Monod, J. Phys. Chem. Solids **28**, 1261 (1967).
[6] A.S. Ivanov *et al.*, Fiz. Nizk. Temp. **17**, 1303 (1991) [Sov. J. Low Temp. Phys. **17**, 695 (1991)].
[7] V.M. Bobetic, Phys. Rev. **136**, A1535 (1964).
[8] H.G. Schuster, Solid State Commun. **13**, 1559 (1973).
[9] J.D. Axe, G. Shirane, Phys. Rev. Lett. **30**, 215 (1973).
[10] S.M. Shapiro, G. Shirane, and J.D. Axe, Phys. Rev. B **12**, 4899 (1975).
[11] F. Marsiglio, Phys. Rev. B 47, 5419 (1993); in *Lattice Effects in High-T_c Superconductors*, edited by Y. Bar-Yam, T. Egami, J. Mustre-de Leon, and A.R. Bishop (World Scientific, Singapore, 1992), p. 157.
[12] F. Stern, Phys. Rev. Lett. **18**, 546 (1967).
[13] M.S. Hybertsen *et al.*, Phys. Rev. B **41**, 11068 (1990).
[14] L. Pintschovius *et al.*, in *International Seminar on High-Temperature Superconductivity*, edited by V.L. Aksenov *et al.* (World Scientific, New Jersey, 1990).
[15] J.P. Hurault, J. Phys. (Paris) **26**, 252 (1965).
[16] See J.R. Schrieffer, *The Pairing Theory of Superconductivity* (Addison-Wesley, New York, 1964).
[17] G.D. Mahan, *Many-Particle Physics* (Plenum, New York, 1990).
[18] H. Krakauer, W.E. Pickett, and R.E. Cohen, Phys. Rev. B **47**, 1002 (1993).
[19] D.A. Papaconstantopoulos, W.E. Pickett, and M.J. DeWeert, Phys. Rev. Lett. **61**, 211 (1988).
[20] M.E. Flatté, Phys. Rev. Lett. **70**, 658 (1993).
[21] M.E. Flatté, S. Quinlan, and D.J. Scalapino, Phys. Rev. B **48**, 10 626 (1993).

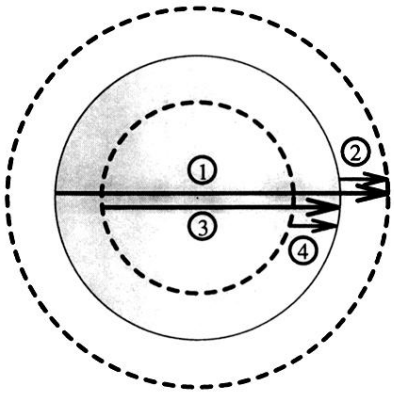

FIG. 2. Four possible extremal excitations for a fixed ω. The two dashed lines are energy contour surfaces at $\hbar\omega$ below and above the Fermi surface, indicated by the solid circle. For momenta greater than (1) and (3) there are no real single-pair excitations of the Fermi sea of this type. For momenta smaller than (2) and (4) there are no single-pair excitations of this type.